2-1-2021

Evaluation of crop coefficient and evapotranspiration data for sugar beets from landsat surface reflectances using micrometeorological measurements and weighing lysimetry

Tianxin Wang

Forrest S. Melton

Isabel Pôças

Lee F. Johnson

Touyee Thao

See next page for additional authors

Authors

Tianxin Wang, Forrest S. Melton, Isabel Pôças, Lee F. Johnson, Touyee Thao, Kirk Post, and Florence Cassel-Sharma

Agricultural Water Management 244 (2021) 106533

Contents lists available at ScienceDirect

Agricultural Water Management

journal homepage: www.elsevier.com/locate/agwat

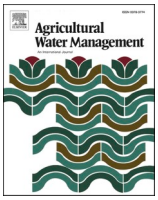

Review

Evaluation of crop coefficient and evapotranspiration data for sugar beets from landsat surface reflectances using micrometeorological measurements and weighing lysimetry

Tianxin Wang [a,b,c,*], Forrest S. Melton [a,b], Isabel Pôças [d], Lee F. Johnson [a,b], Touyee Thao [e], Kirk Post [a,b], Florence Cassel-Sharma [e]

[a] Cooperative for Research in Earth Science and Technology, NASA Ames Research Center, Moffett Field, CA, USA
[b] California State University, Monterey Bay, Department of Applied Environmental Science, Seaside, CA, USA
[c] University of California, Berkeley, Department of Environmental Science, Policy, and Management, Berkeley, CA, USA
[d] Centre For Research in Geo-Space Science (CICGE), Porto, Portugal
[e] California State University, Fresno, Department of Plant Science, Fresno, CA, USA

ARTICLE INFO

Handling Editor - Dr. N. Jovanovic

Keywords:
Crop coefficient
Crop evapotranspiration (ET_c)
Actual crop evapotranspiration (ET_a)
Eddy covariance
Energy balance residual
Remote sensing

ABSTRACT

In California and other agricultural regions that are facing challenges with water scarcity, accurate estimates of crop evapotranspiration (ET_c) can support agricultural entities in ongoing efforts to improve on-farm water use efficiency. Remote sensing approaches for calculating ET_c can be used to support wide area mapping of crop coefficients and ET_c with the goal of increasing access to spatially and temporally distributed information for these variables, and advancing the use of evapotranspiration (ET) data in irrigation scheduling and management. We briefly review past work on the derivation of crop coefficients and ET_c data from satellite-derived vegetation indices (VI) and evaluate the accuracy of a VI-based approach for calculation of ET_c using a well instrumented, drip irrigated sugar beet (*Beta vulgaris)* field in the California Central Valley as a demonstration case. Sugar beets are grown around the world for sugar production, and are also being evaluated in California as a potential biofuel crop as well as for their ability to scavenge nitrogen from the soil, with important potential benefits for reduction of nitrate leaching from agricultural fields during the winter months. In this study, we evaluated the accuracy of ET_c data from the Satellite Irrigation Management Support (SIMS) framework for sugar beets using ET data from a weighing lysimeter and a flux station instrumented with micrometeorological instrumentation. We used the Allen and Pereira (A&P) approach, which was developed to estimate single and basal crop coefficients from crop fractional cover (f_c) and height, and combined with satellite-derived f_c data and grass reference ET (ET_o) data as implemented within SIMS to estimate daily ET_c from SIMS ($ET_{c\text{-}SIMS}$) for the sugar beet crop. The accuracy of the daily $ET_{c\text{-}SIMS}$ data was evaluated against daily actual ET data from the weighing lysimeter ($ET_{a\text{-}lys}$) and actual ET calculated using an energy balance approach from micrometeorological instrumentation ($ET_{a\text{-}eb}$). Over the course of the 181-day production cycle, $ET_{c\text{-}SIMS}$ totaled 737.1 mm, which was within 7.7% of total $ET_{a\text{-}lys}$ and 3.7% of $ET_{a\text{-}eb}$. On a daily timestep, SIMS mean bias error was −0.31 mm/day relative to $ET_{a\text{-}lys}$, and 0.15 mm/day relative to $ET_{a\text{-}eb}$. The results from this study highlight the potential utility of applying satellite-based f_c data coupled with the A&P approach to estimate ET_c for drip-irrigated crops.

1. Introduction

The California agricultural community is facing challenges related to the increasing interannual variability of precipitation and constraints on water resources. In response to sustained declines in groundwater levels and the extreme drought that began in 2011 and extended through 2016, the Sustainable Groundwater Management Act (SGMA) was passed by the California Legislature in 2014 to regulate overdraft of aquifers and increase the sustainability of groundwater supplies. Additionally, in 2012, groundwater regulations were added to the Irrigated Lands Regulatory Program in California to prevent agricultural runoff and leaching of fertilizers from irrigated fields from impacting surface

* Correspondence to: Chapman Science Academic Center, 100 Campus Center, Seaside, CA 93955, USA.
E-mail address: cawang@csumb.edu (T. Wang).

https://doi.org/10.1016/j.agwat.2020.106533
Received 3 February 2020; Received in revised form 11 September 2020; Accepted 21 September 2020
Available online 3 October 2020

and groundwater resources. These policies have led to increased interest among the agricultural community in adopting new information technologies to support data driven approaches in irrigation management and scheduling, with the goal of evaluating and potentially increasing on-farm water use efficiency.

The Food and Agriculture Organization Irrigation and Drainage Paper 56 (FAO56) synthesized decades of research to provide a framework and methodology for computing crop water requirements though the integration of reference evapotranspiration calculated from meteorological data and crop coefficients (Allen et al., 1998). FAO56 provides look-up tables and equations to support calculation of crop coefficients (K_c) for a wide range of crops at different growth stages. FAO56 includes both single K_c and dual K_c approaches. In the dual K_c approach, the K_c value is determined through separate calculation of a basal crop coefficient (K_{cb}) and a soil evaporation coefficient (K_e). K_{cb} is defined as evapotranspiration from a well-watered crop with a dry soil surface. K_{cb} is used primarily to represent the transpiration component of ET, but also includes diffusive soil evaporation, while K_e is used to capture evaporation from exposed soil. K_{cb} and K_e are summed to calculate the dual-K_c value, which is then multiplied by the reference ET calculated using the Penman–Monteith equation from meteorological measurements obtained over a reference crop, typically a well-watered 0.12 m grass surface (ET_o). Crop water stress can also be accounted for in this approach via incorporation of a stress coefficient (K_s) calculated using a soil water balance model. During the initial crop development period, evaporation from exposed soil typically accounts for the majority of ET_c. As the crop canopy develops, evaporation from exposed soil decreases while the transpiration increases and eventually becomes the dominant process (Allen et al., 1998).

Satellite observations enable estimation of crop water requirements on a regional scale with good spatial (30 m) and temporal (5–8 days) resolution (Kjaersgaard et al., 2011). By providing near real time measurements of crop conditions through remote sensing at the scale of individual fields, information can benefit growers by allowing them to accurately and easily monitor the crop canopy development and the crop water requirements (Trout et al., 2008). Previous studies have used remote sensing on various crops to estimate K_c and K_{cb} values from vegetation indices (VIs), such as the Normalized Difference Vegetation Index (NDVI) and the Enhanced Vegetation Index (EVI), calculated from satellite top of atmosphere (TOA) reflectance or surface reflectance data, and these results have demonstrated the potential value for the agricultural community of operational systems (Glenn etal.,2007; Pôças et al., 2020). Previous work related specifically to sugar beets using VIs approach is limited, however, and includes a study by González-Dugo and Mateos (2008) that used satellite observed VIs to obtain K_{cb} values for sugar beets in Spain. Their study concluded that there was value in using satellite VI data to estimate K_{cb} values, but did not evaluate the accuracy of the K_{cb} or ET_c data. Instead, the study focused on evaluation of crop yields and water productivity. Tasumi and Allen (2007) also applied remote sensing and an energy balance model, the Mapping Evapotranspiration with Internalized Calibration (METRIC) model, to estimate K_c values for sugar beets and other major crops grown in Idaho.

In the U.S., sugar beet (Beta vulgaris) is a valuable crop grown commercially with the purpose of producing sugar and biofuel (Panella et al., 2015). Kaffka et al. (2014) described key factors in California that enable the suitability and potential of sugar beets for biofuel production. Under the Energy Independence and Security Act (EISA) of 2007, sugar beet was qualified as a potential feedstock for advanced biofuel production with the potential for greenhouse gas reductions of up to 50% (110th Congress, 2007). Due to the high sugar content, beets could potentially double ethanol production compared to other feedstocks (Panella and Kaffka, 2010). Furthermore, sugar beet processing by-products can serve as a soil amendment for nitrate reduction (Kumar et al., 2002).

As the use of satellite-based models for estimating ET becomes more common, it is important to have robust ground-based measurements across a range of crop types and growth forms that can be used to evaluate remotely sensed ET. Surface reflectance-based models typically use information in the visible and near-infrared (VNIR) wavelengths to estimate K_c or K_{cb}, and then combine these values with daily ET_o values derived from meteorological data to calculate ET_c following the FAO56 approach. Many previous studies have investigated the relationship between K_c or K_{cb} and VIs (Bausch and Neale, 1987; Bausch, 1993; Benedetti and Rossini, 1993; Hunsaker et al., 2003a, 2003b, 2005; Glenn et al., 2011), and Pôças et al. (2020) provide a recent review of the literature on this topic. Thermal-based remote sensing approaches use thermal infrared (TIR) measurements to solve energy balance equations to estimate ET (e.g., Allen et al., 2007; Bastiaanssen et al., 1998; Kustas et al., 2004). While there has been important recent progress on automation of energy balance models for field scale applications (Allen et al., 2007; Semmens et al., 2016), sustained operational production of daily ET estimates from energy balance approaches remains challenging. VI-based approaches for field-scale ET_c mapping have a few key advantages for irrigation management applications. First, moderate resolution (10–300 m) VNIR measurements are available from a large constellation of satellite and airborne sources (Murray et al., 2009; Calera et al., 2017), increasing the temporal resolution of the satellite measurements. Second, the algorithms used in the models are computationally simpler and avoid the need for internal or scene-by-scene calibration (Rafn et al., 2008), facilitating automated data processing over large areas and reducing data latency, which is critical for irrigation management applications. Third, VNIR observations are available at higher spatial resolution compared to thermal based remote sensing for individual fields (Johnson and Trout, 2012), increasing the utility and accuracy for smaller fields without the need for pan-sharpening or data fusion.

One important limitation of VI-based approaches is that they typically estimate ET_c assuming well-watered conditions, and they are less sensitive to intermittent deficit irrigation and short-term crop stress, which can lead to overestimation of actual ET for deficit irrigated crops (Glenn et al., 2011). For irrigation management applications, however, estimation of ET_c assuming well-watered conditions provides a consistent reference for the irrigator, making it easier to adjust irrigation management to meet their production goals. In contrast, measurement of actual ET (ET_a) requires the irrigator to use additional information to determine whether the ET_a represents stressed or unstressed conditions, and then make corrections to calculate ET_c as the baseline for an intentional deficit irrigation regime.

A second limitation of VI-based approaches is that they are less sensitive to evaporation from bare soil, and require integration with a soil water balance model to estimate soil evaporation (González-Dugo and Mateos, 2008; Melton et al., 2012). While this can be an important limitation for estimation of evaporation from bare soil or sparsely covered fields during the winter, the period during which soil evaporation is a significant percentage of total ET_c during active crop production is typically limited to a few weeks. A key objective in this study was to determine how well ET_c from a VI-based approach compared to ground-based measurements, and to characterize the overall impact of these two limitations on the accuracy of the ET_c estimates.

Glenn et al. (2011) evaluated different VI-based methods used in ET studies and provided evidence that this method can be applied to acquire accurate estimates of ET. Of the various VIs, the Normalized Difference Vegetation Index (NDVI) is a widely used measure of vegetation density and condition (Goward et al., 1991). One of the earliest applications of a VI-based approach was described by Bausch and Neale (1987) and this study found that NDVI was highly correlated with leaf area index (LAI) and f_c. These authors proposed a linear transformation between NDVI and K_{cb} to represent a reflectance-based crop coefficient (K_{cb}-VI) which tracked closely with K_c measured by the weighing lysimeter. This study concluded that the K_{cb}-VI approach could be used to schedule irrigation at field scales. The K_{cb}-VI method has also been applied to numerous other crops, yielding the conclusions that: 1) The

use of NDVI as a supplement to static K_{cb} values can improve on farm water management (Hunsaker et al., 2007a, 2007b; Samani et al., 2009); and, 2) $K_{cb\text{-}VI}$ also gave consistently accurate results and highlighted the potential to improve irrigation when plants are under aberrant conditions compared to those represented by conventional FAO56 approaches (Hunsaker et al., 2003a, 2003b, 2005).

Close correlation is commonly established between vegetation amount and transpiration, where, as vegetated cover increases, transpiration increases (Glenn et al., 2007). Based on the strong relationship between NDVI and K_{cb}, Trout et al. (2008) and Johnson and Trout (2012) investigated the relationship between satellite derived NDVI and ground measured fractional cover (f_c), the proportion of ground that is covered with green vegetation. Johnson and Trout (2012) used a multispectral camera to measure the fc of 49 commercial fields that contained 18 different crop types over 11 Landsat overpass dates. They found that the Landsat NDVI formed a strong linear relationship with measured fc, supporting the use of satellite-derived NDVI to calculate fc for agricultural crops.

Due to the cost-effectiveness and flexibility of satellite data, remote sensing has been implemented to map K_c and K_{cb} values and estimate ET on field and regional scales. Building on the studies described above, Melton et al. (2012) developed the Satellite Irrigation Management Support (SIMS) framework, which integrates satellite data and meteorological data from the California Irrigation Management Information System (CIMIS) (Hart et al., 2009) to provide data for NDVI, f_c, K_{cb}, and ET under well-watered conditions with a dry soil surface, which we notate as $ET_{c\text{-}SIMS}$. $ET_{c\text{-}SIMS}$ largely represents the transpiration component of ET. However, SIMS does set K_{cb} at a minimum of 0.15 to account for baseline evaporation from bare soil and includes diffusive soil evaporation (Melton et al., 2012). In addition, SIMS K_{cb} values can be combined with a soil water balance model to calculate soil evaporation coefficients (K_e) and crop stress coefficients (K_s), following the FAO56 dual crop coefficient approach (Allen et al., 1998). SIMS was developed to support irrigation management and regional water accounting, to help irrigators and water managers account for interannual variability and heterogeneity in field conditions. Various studies have discussed the importance of adjusting tabulated K_c and K_{cb} values provided by FAO56 based on local conditions and climate variability (Pereira et al., 2015; Drerup et al., 2017). A brief overview of SIMS is provided in Section 2.2, and detailed information about the SIMS algorithms and workflow can be found in Melton et al. (2012, 2020), and a full description of the Allen and Pereira (A&P) equations encoded within SIMS is provided in Pereira et al. (2020).

In a recent study, Melton et al. (2018) described the improvements of SIMS, summarized work to date quantifying the accuracy of $ET_{c\text{-}SIMS}$, and demonstrated the operational use of SIMS to improve irrigation management. Melton et al. (2018) also conducted an accuracy assessment with in-situ measurements over a dozen crop types in California. Results showed that seasonal $ET_{c\text{-}SIMS}$ estimates are within 9% mean absolute error (MAE) of measured crop evapotranspiration for well-watered crops, and 15% MAE across all crops studied, including deficit irrigated crops such as wine grapes and cotton.

Glenn et al. (2011) found that discrepancies between ET calculated from satellites and ground-based instrumentation can range from 5% to 10% for lysimetry and 10–30% for open path eddy covariance. Here, we refer to data from the satellite-based approach as the "modeled" data, and the ET calculated from the ground-based observations as the "measurements", recognizing that the ET data from the ground-based instrumentation also has errors and uncertainty, and involves application of biophysical and micrometeorological models to calculate ET values from the measurements collected on the ground (Glenn et al., 2011). It is important to distinguish that actual ET, from weighing lysimeter ($ET_{a\text{-}lys}$) and flux station ($ET_{a\text{-}eb}$), stands for ET calculated directly from measurements collected by instruments and includes soil evaporation and canopy transpiration, as well as the impact of any crop water stress. Differently, $ET_{c\text{-}SIMS}$ is determined from the combination of satellite-VI derived K_{cb} and ET_o. $ET_{c\text{-}SIMS}$ does not account for soil evaporation and crop water stress unless it results in a reduction in biomass or crop geometry change, hence, a key question addressed by this study is the ability of $ET_{c\text{-}SIMS}$ to accurately estimate ET despite these limitations. As discussed by various studies, when using VI-based approaches for estimating and mapping ET_c, a soil water balance model for the surface layer and the root zone may be utilized to further increase the accuracy of ET_c estimates if soil evaporation or crop water stress are major considerations (Campos et al., 2013; Mateos et al., 2013; Pôças et al., 2015; Odi-Lara et al., 2016).

The objective of this paper is to assess the accuracy and applicability of a VI-based remote sensing model that incorporates the A&P approach to estimate ET_c in sugar beets. We also evaluated the accuracy of the $ET_{a\text{-}eb}$ measurements against $ET_{a\text{-}lys}$ measurements to evaluate the utility of using an energy balance residual approach for measurement of latent energy fluxes from a flux station. Our strategy in this assessment was to quantify each independently calibrated measurement that occurred simultaneously at the same location to evaluate the potential utility of the VI-based remote sensing approach used by SIMS for estimation of ET_c for drip-irrigated sugar beets.

2. Methods

2.1. Study site

The sugar beet field is located in Five Points, CA (Lat: 36.3379, Long: −120.1131, Elev: 82.0 m) at the West Side Research and Extension Center (WSREC) with average annual precipitation of 175 mm. The site has a flat terrain with a Mediterranean climate of cool, wet winters and warm, dry summers. The prevailing wind comes from the northwest (Fig. 1) and the soil type at the site is Panoche clay loam (Typic Torriorthents).

The beets were planted on Oct 22, 2014 with a 0.15 m spacing between plants and a 0.02 m seeding depth. The field was 106 m (348 ft) long and 61 m (200 ft) wide with 140 rows oriented ~1 degree northwest. The field was irrigated with sprinklers prior to planting, through germination and the early stages of crop development, and then the irrigation switched to surface drip irrigation on Jan 2nd, 2015. Irrigation was measured in the field using flow meters (Badger Meter, Milwaukee, WI, USA) installed on two drip laterals in the field, as well as from measurements recorded by the weighing lysimeter. For the study period from Jan 1st to June 30th, 2015, the field was irrigated 2–3 times per week using the surface drip irrigation system and a total of 659 mm of water was applied (Fig. 1). The WSREC staff managed the irrigation scheduling based on data from the weighing lysimeter located in the field. California Irrigation Management Information System (CIMIS) weather station #2 was used to obtain ET_o data. This weather station (Lat: 36.336222, Long: −120.112910, Elev: 86.9 m) is located inside the WSREC field station and installed over a well-watered grass field. The field was harvested August 4th, 2015.

2.2. Remotely sensed data

The Satellite Irrigation Management Support (SIMS) system was developed to support mapping of crop development and crop water demand throughout California (Melton et al., 2012). SIMS uses satellite-derived surface reflectances to map NDVI, f_c, and K_{cb} (basal crop coefficients). To calculate the daily $ET_{c\text{-}SIMS}$, K_{cb} is combined with daily ET_o data from the California Department of Water Resources California Irrigation Management Information System (CIMIS).

SIMS can be driven with satellite data from multispectral instruments onboard satellites including Landsat 5, Landsat 7, Landsat 8, Sentinel-2A, Sentinel-2B and others that collect measurements in the VNIR wavelengths. For the comparisons with ground measurements of ET described below, atmospherically corrected surface reflectance data were obtained from the USGS Landsat Collection 1 for the Operational

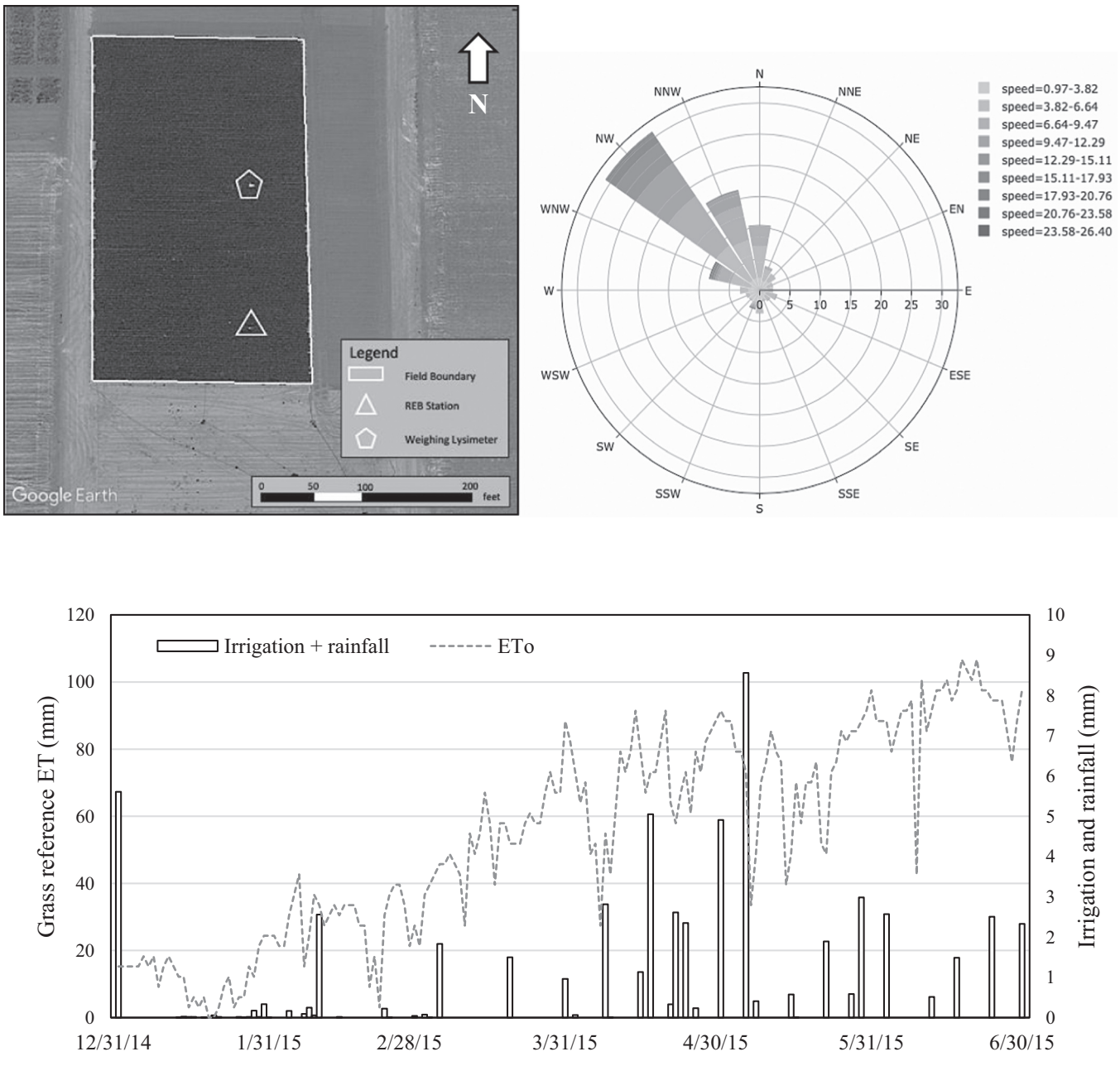

Fig. 1. (top-left): Field diagram showing the location of the weighing lysimeter and REB station during the 2015 growing season. Image date: 2015/05/02. (top-right): Windrose of the study site with the wind speed in miles per hour. (bottom): Irrigation and rainfall, and grass reference ET (ET_o).

Land Imager (OLI) on Landsat 8. Landsat 7 and Landsat 8 each have a 16-day revisit interval, but since they are staggered, one observation is available approximately every 8-days. Due to overlap in the scene boundaries, Landsat observations are available more frequently for some locations, as was the case for our field site. SIMS uses the highest quality, cloud-free observations for each pixel and composites them into a mosaic every eight days. In cases where data is available from both Landsat 7 and Landsat 8, Landsat 8 is given priority. Due to the fact that our study site is located within the overlap between Path 42 and Path 43, we were able to obtain one Landsat 8 scene almost every 8 days excepting cloud cover. Landsat scenes used in this study can be found in Table 1.

Table 1
Landsat scenes acquired and used in the analysis.

Path	Row	Landsat 7 acquired dates	Landsat 8 acquired dates
42	35	/	19-Feb-2015, 07-Mar-2015, 08-Apr-2015, 10-May-2015, 26-May-2015, 11-Jun-2015, 27-Jun-2015, 13-Jul-2015, 29-Jul-2015
43	35	Jan-1–2015	26-Feb-2015, 14-Mar-2015, 30-Mar-2015, 15-Apr-2015, 01-May-2015, 02-Jun-2015, 18-Jun-2015, 04-Jul-2015, 20-Jul-2015, 05-Aug-2015

2.3. Calculation of $ET_{c\text{-}SIMS}$ from satellite data and CIMIS ET_o

SIMS first calculates NDVI values from surface reflectance values as:

$$NDVI = \frac{NIR - R}{NIR + R} \quad (1)$$

Where NIR is the reflectance in the near-infrared wavelengths, and R is the reflectance in the red wavelengths. NDVI is then linearly interpolated between cloud-free satellite overpass dates to calculate a daily timeseries (Fig. 2). Next, SIMS applies the equation described in Trout et al. (2008) and Johnson and Trout (2012) to map f_c from NDVI at a spatial resolution of 30 m x 30 m per pixel following Eq. (2):

$$f_c = 1.26 * NDVI – 0.18 \quad (2)$$

SIMS calculates K_{cb} values via the f_c values (Fig. 2) calculated from the satellite observation using Eq. (2) and a density coefficient (K_d) derived from a biophysical description of the canopy. This approach follows Allen and Pereira (2009), Eq. (10):

$$K_d = \min\left(1, M_L * f_{ceff}, \quad f_{c\ eff}^{(1/(1+h))}\right) \quad (3)$$

where, $f_{c\ eff}$ is the effective fraction of ground covered or shaded by vegetation, h is the crop height (Fig. 2), and M_L is a canopy radiation transparency factor ranging from 1.5 to 2.0 (Allen and Pereira, 2009; Pereira et al., 2020). K_d links increase in K_{cb} to increasing vegetation amount. Details of calculations of crop height are provided in Pereira et al. (2020, this issue) and in the SIMS User Manual (Melton et al., 2020). For this study, we used a M_L of 2.0 for sugarbeet. As a simplifying assumption to facilitate full automation, the current release of SIMS assumes standard climate conditions.

$K_{cb\ full}$, which represents conditions at peak plant growth for conditions having nearly full ground cover, is calculated as a simplified version of Eq. 7a of Allen and Pereira (2009):

$$K_{cb\ full} = F_r * (\min(1.0 + 0.1h_{max}, 1.2)) \quad (4)$$

where F_r (range 0–1) is an adjustment factor related to stomatal regulation. For annuals, F_r is assigned a standard value of 1. For perennials, which tend to exhibit more stomatal control on transpiration, F_r is < 1 and varies by crop type and seasonal growth stage (Allen and Pereira, 2009; Pereira et al., 2020). For this study, we used a F_r of 1.0 fo_r sugarbeet.

K_{cb} is then derived following Eq. (5a) from Allen and Pereira (2009):

$$K_{cb-SIMS} = K_{cb\ min} + K_d * \left(K_{cb\ full} – K_{cb\ min}\right) \quad (5)$$

where $K_{cb\ min}$ is set to 0.15, which is the minimum K_{cb} value for bare soil under typical agricultural conditions (Allen and Pereira, 2009). Values of h_{max} are drawn from Table 12 of FAO56 (Allen et al., 1998). Values for h are estimated for annual crops as a linear function of f_c and h_{max}. For tree and vine crops, values from Table 11 of FAO56 are used for the late stage start and stop dates.

As a final step, SIMS calculates $ET_{c\text{-}SIMS}$ following the FAO56 dual crop coefficient approach (Allen et al., 1998), as:

$$ET_{c-SIMS} = (K_{cb-SIMS} + K_e) * ET_o \quad (6)$$

Where K_{cb} is the SIMS basal crop coefficient calculated from Eq. (5), K_e is the soil evaporation coefficient, and ET_o is the grass reference ET. Due to

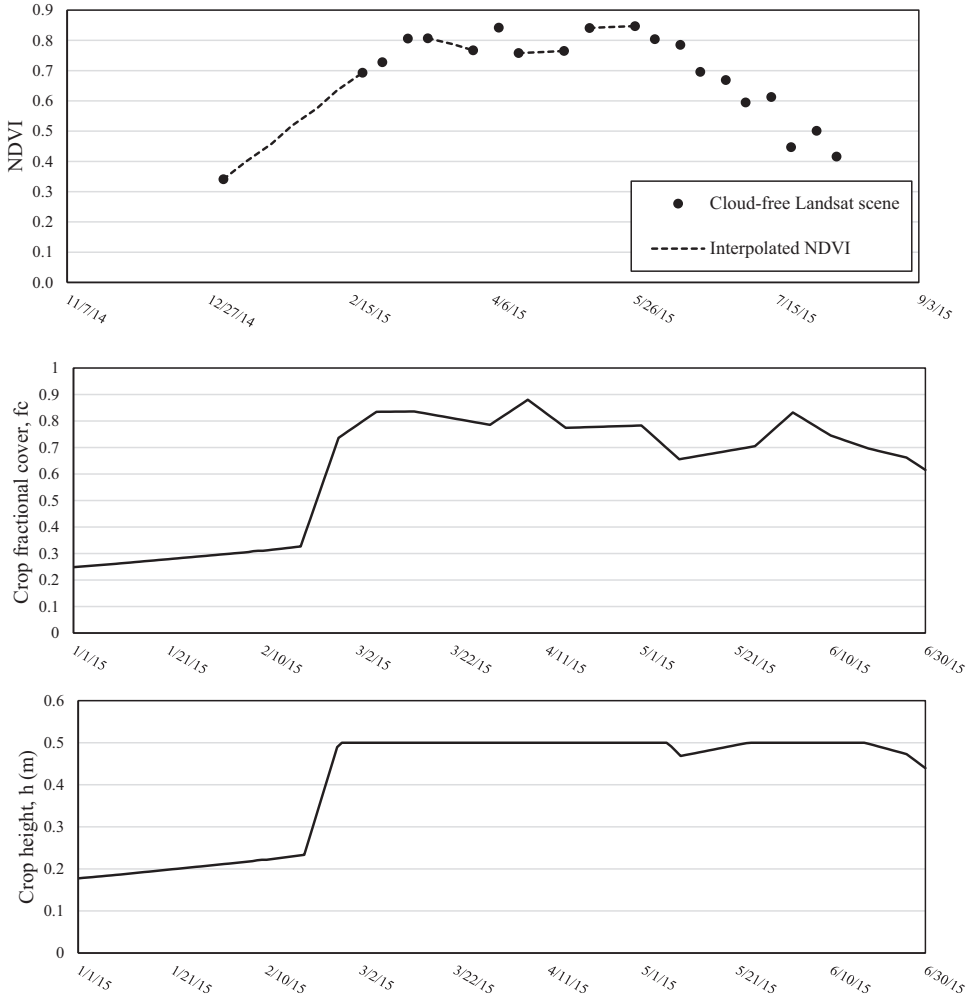

Fig. 2. Timeseries of NDVI from Landsat (top), fraction cover from SIMS (middle), and crop height from SIMS (bottom) for the sugar beet field.

the fact that reflectance-based approaches are less sensitive to evaporation from exposed soil, in Eq. (6) SIMS was originally developed to estimate K_{cb} and currently must set the evaporation coefficient (K_e) as equal to zero for wide area mapping ET applications. In a drip irrigated system with lines shaded by vegetation, as in the present study, this simplification is acceptable. Ongoing work will enhance SIMS to include a gridded soil water balance model to support calculation of K_e. For this study, ET_o was obtained from Spatial CIMIS (Hart et al., 2009) operated by the California Department of Water Resources. While the Spatial CIMIS data was used in this study, outside of California SIMS utilizes ET_o data from gridMET (Abatzoglou and Ficklin, 2017). Additional details on the A&P approach and SIMS algorithms and documentation can be found in Pereira et al. (2020) and Melton et al. (2020), respectively.

2.4. Weighing lysimeter

This site has a weighing lysimeter located in the center of the field consisting of a 2-m by 2-m by 2.25-m deep soil tank positioned on a mechanical tank scale (Model FS-4; Cardinal Scale Manufacturing Co., Webb City, MO) that is housed underground. Due to limitations on the lysimeter's accessibility by tractors, the lysimeter plot was hand planted following the same scheme as the rest of the field. The soil and plants in the lysimeter were irrigated from a supply tank located underneath the lysimeter each time the lysimeter weight decreased by 4 kg (i.e., 1 mm of water). On a daily basis, ET was monitored and computed through the weight change in the soil tank via the 91 kg capacity stainless steel "S" beam load cell (Omega Engineering Inc., Norwalk, CT). The data were logged onto a CR3000 datalogger (Campbell Scientific Inc., Logan, UT) once every 60 s. The accuracy of the weighing lysimeter measurements is controlled through calibration. In this study, the calibration was done by using a known weight (40–200 kg) on the surfaces of the lysimeter. Additionally, two 0.3 kg weights were used to ensure detections of small changes. The load cell then recorded and averaged three readings (mV) for each known weight. Last, a linear regression, between load cell readings (x-axis) and weights (y-axis), was determined and incorporated into the lysimeter's program. Besides the factory calibration in Jan 2014, two additional calibrations were conducted, on Dec 23rd, 2014 and Feb 18th, 2015, to validate and ensure the accuracy of the weighing lysimeter. Both calibrations produced very high coefficient of determination values (R^2) with 0.9999 for 2014 and 0.9998 for 2015, indicating a high level of accuracy of the weighing lysimeter.

The theory and details of the weighing lysimeter are well documented in the literature, and details can be found in Bryla et al. (2010). Specific details for the lysimeter used in this study are described in Thao (2017).

2.5. Flux measurements

Open path eddy covariance (OPEC) is an approach that uses measurements collected by micrometeorological instrumentation to calculate ET. The OPEC approach has been extensively used to estimate actual crop evapotranspiration (ET_a) and validate remote sensing models (Moorhead et al., 2019). Full OPEC instrumentation includes both a 3D sonic anemometer and an infrared gas analyzer. As a result, it is quite expensive and many studies have also explored use of the residual of the energy balance (REB) approach, which also uses a 3D sonic anemometer but does not require use of an infrared gas analyzer. The REB approach applies the energy balance equation (Eq. 8) to estimate latent heat flux density as the residual with a forced energy balance closure (Twine et al., 2000), and this micrometeorological measurement is mainly implemented over vegetated regions (Pan et al., 2017). Anapalli et al. (2018) used the REB approach in a cotton and a corn field. In the cotton field, which also had a large-scale field lysimeter, they found that ET measured from the flux data compared well with ET measured in the lysimeter yielding a RMSE for daily ET of 1.2 mm and a seasonal ET error within 1%. In the corn field, they found a strong correlation between ET measured from the flux data and reference ET data for alfalfa and grass with Pearson's correlation coefficients of 0.81 and 0.70, respectively. Their results demonstrated that the REB procedure is a possible alternative method for calculation of actual ET from micrometeorological instrumentation, and a cost-effective alternative to ET_a measurements from lysimetry and OPEC systems.

Flux measurements require enough fetch, the horizontal distance from sensor to predominant wind direction, to achieve representative measurements from an area of interest. A general rule of thumb requires a fetch to measurement height ratio of 100:1, over a homogenous and flat surface with no sudden changes in landcover (Businger, 1986; Gash, 1986; Horst and Weil, 1994; Tanner, 1988). However, Burba (2001) conducted EC measurements over a tallgrass prairie and found that over 80% of the latent heat flux came from 80 m within the predominant wind for a measurement height of 1.5 m. Additionally, they examined the effect of roughness on fetch and found that the largest contribution of latent heat flux came from 12 to 18 m and 30–35 m of predominant wind distance for high (canopy height of 0.6 m) and low (canopy height < 0.05 m) roughness, respectively.

In this study, the REB station, following the approach described by Linquist et al. (2015), was deployed to estimate latent heat flux density and calculate the $ET_{a\text{-}eb}$ from the residual of the energy balance. One limitation of the REB approach is that it does not provide a direct measurement of latent heat fluxes via an infrared gas analyzer and a sonic anemometer and instead derives the latent heat flux through the residual. As a result, the energy balance closure, as described in Twine et al. (2000), is not determinable. Our study site has a flat terrain with a predominant wind from the northwest with a secondary contribution from north-northwest (Fig. 1). Due to the small size of the area of study, a ratio of 100:1 is restricted. To best ensure a sufficient fetch while avoiding edges of the field, we placed the station about 90 m from the predominant wind as shown in Fig. 1.

The assembly of the station was based on procedures described by McElrone et al. (2013). All data were logged and stored in a datalogger (CR1000, Campbell Scientific Inc., Logan, UT). A data logger program was used for data acquisition and post-processing following the steps described in Shapland et al. (2013). The station was maintained and adjusted weekly so that all sensors were clean and functioning properly.

2.5.1. Net radiation and ground heat flux density

A two-way net radiometer (NR Lite 2 Net Radiometer, Kipp & Zonen, Delft, Netherlands) was maintained at 2 m above the canopy to measure net radiation (R_n), the total incoming radiation minus the total outgoing radiation. Six soil heat flux plates (REBS HFT3 Heat Flux Plate, REBS, Inc., Seattle, WA, USA) were buried at a depth of 5 cm. Each plate was paired with soil thermocouple probes (TCAV Soil Thermocouple Probe, Campbell Scientific, Inc., Logan, UT, USA), installed on either side of the plate, with one probe installed diagonally from a depth of 5–2 cm, and the second probe installed diagonally from 2 cm to 5 cm. Six capacitance probes (Decagon 10HS, Meter Group, Pullman, WA, USA) were also installed near each soil heat flux sensor package at a depth of 5 cm to measure volumetric water content. These sensors provided measurements of ground heat flux (G) that included the soil heat flux across the heat flow transducer (G_T) and change in heat storage in the soil layer above the transducers (ΔS), such that $G = G_T + \Delta S$ (Shapland et al., 2013).

2.5.2. Sensible heat flux density from eddy covariance

A three-dimensional ultrasonic anemometer (81000 3D Sonic Anemometer, RM YOUNG, Traverse City, MI, USA) was maintained at 1.5 m above the canopy to collect wind velocity and sonic temperature, with a sampling frequency of 10 Hz, to measure sensible heat flux density (H) from the sonic anemometer via the covariance of the vertical wind and the sonic temperature (Eq. 7, Swinbank, 1951):

$$H = \rho_a C_p \left(\overline{w' T_s'}\right) \quad (7)$$

Where ρ_a is the air density (g m^{-3}), C_p is the specific heat of air at constant pressure (J g^{-1} K^{-1}), w is the speed of vertical wind component (m s^{-1}), and T_s is the sonic temperature (K). $\overline{w' T_s'}$ is the covariance between the vertical wind component and the sonic temperature with a two-dimensional coordinate rotation (Tanner and Thurtell, 1969). A two-dimensional rotation is also implemented within the logger program (Meyers and Baldocchi, 2005).

2.5.3. Latent heat flux density and evapotranspiration

The latent heat flux density, an indirect measurement, is determined from the residual of the energy balance (Twine et al., 2000):

$$\lambda E = R_n - G - H \quad (8)$$

Where λE is the latent heat flux density (MJ m^{-2}), R_n is the net radiation (MJ m^{-2}), G is the ground heat flux density (MJ m^{-2}), and H is the sensible heat flux density (MJ m^{-2}). All flux densities were converted from W m^{-2} to MJ m^{-2} for the calculation above, with gap-filling via linear interpolation applied prior to being used in the calculation of λE. These instantaneous (half-hourly) λE were then computed into daily profiles. The mass flux density of water vapor, ET (mm), is then determined as:

$$ET = \frac{\lambda E}{\lambda} \quad (9)$$

Where λ is the latent heat of evaporation, which equals 2.45 MJ per 0.0001 m^3.

3. Results

3.1. Energy balance components

The hourly values (24-h profile) for each of the individual energy balance components throughout the season were averaged to construct the seasonal mean hourly energy balance. The flux densities (R_n and G) usually increased around 6AM and transitioned into stable conditions after 6PM.

During summer in the Central Valley, as the daily average temperature increases throughout the season, we would expect a positive trend in H, similar to R_n and G. However, we observed a decrease in H as the season moved towards summer, suggesting that incoming radiant energy was not the only source of incoming energy. On a finer resolution in Fig. 3, we observed low or negative daytime H (cyan to light green hue) from late May to the beginning of July, which indicates an advection effect, as additional energy other than radiation was added into the system. To investigate this, we evaluated NDVI data around the field throughout the season, to examine the local environmental conditions and assess the potential for advection effects. An example from a Landsat 8 image acquired on June 2nd is shown in Fig. 4. The field is surrounded by pixels with low NDVI, indicating bare, dry soil in the fields adjacent to our study site. One possible reason for the advection effect observed might be that in 2015, as a result of the exceptional drought in California, most of the surrounding fields were left bare and the study field was one of the only irrigated fields at WSREC. With a predominant wind from the NW, the cooler environmental system in the field serves as a sink of energy, as heat transfer will occur spontaneously from higher temperature bodies to lower temperature bodies. During canopy development, more areas were shaded, resulting in cooler soil temperatures, which further increased the field's ability to absorb heat. Consequentially, the additional energy stimulated the growth of λE based on the energy balance presented in Eq. (8).

For periods with negative daily H, in order to avoid uncertainties associated with nighttime fluxes, we used the daytime (6AM–6PM, inclusive) H along with corresponding daytime R_n and G to calculate the residual of the energy balance, instead of using linear interpolation. By using daytime fluxes when daytime H is below zero, the possibility of the field serving as a daytime sink of energy is not neglected, while avoiding the uncertainties with nighttime fluxes. Due to the fact that the closure was forced inherently by the REB approach, it is important that we were able to compare the data from REB station against the weighing lysimeter. This allowed us to assess the accuracy of λE via the comparison with the weighing lysimeter data, which agreed well (Figs. 5 and 6).

3.2. Daily evapotranspiration and intercomparison

3.2.1. Comparisons between methods

All daily ET values collected during the growing season from the flux station, weighing lysimeter, and SIMS were plotted against each other to test the strength of the relationship between measurements (Fig. 5). In addition, statistical metrics for the comparison of daily $ET_{c\text{-}SIMS}$ against $ET_{a\text{-}lys}$ and $ET_{a\text{-}eb}$ were computed (Table 2).

Overall, the results of the comparison between measurements showed good agreement, with R^2 values above 0.9 in all cases. In the comparison between ground measurements, the trendline suggests that a slight underestimation of $ET_{a\text{-}eb}$ relative to $ET_{a\text{-}lys}$ was observed for the lower values of ET_a, while an overestimation occurred for the higher ET_a values. The comparison of daily $ET_{c\text{-}SIMS}$ against $ET_{a\text{-}lys}$ also showed good agreement, with model efficiency (EF) of 0.91, regression coefficient close to 1, MAE of 0.56 mm/day, root mean squared error (RMSE) of 0.73 mm/day, and mean bias error (MBE) of −0.31 mm/day, In the

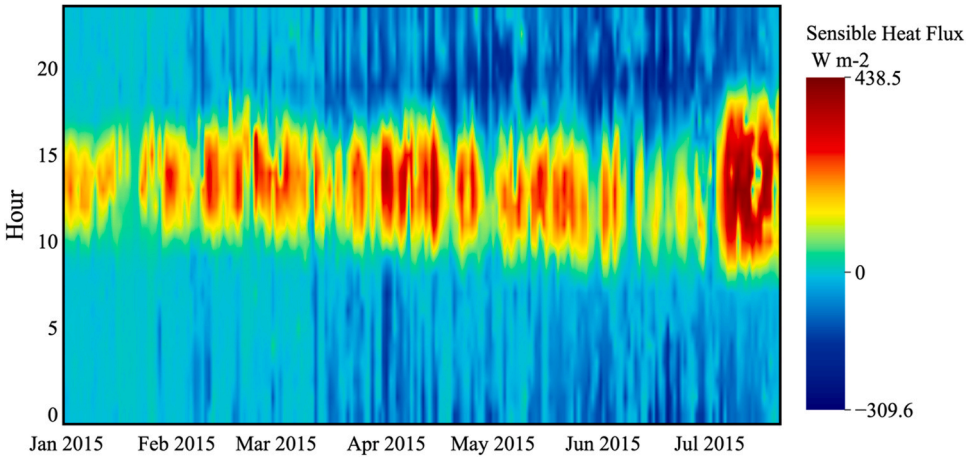

Fig. 3. Distribution of sensible heat flux throughout the growing season.

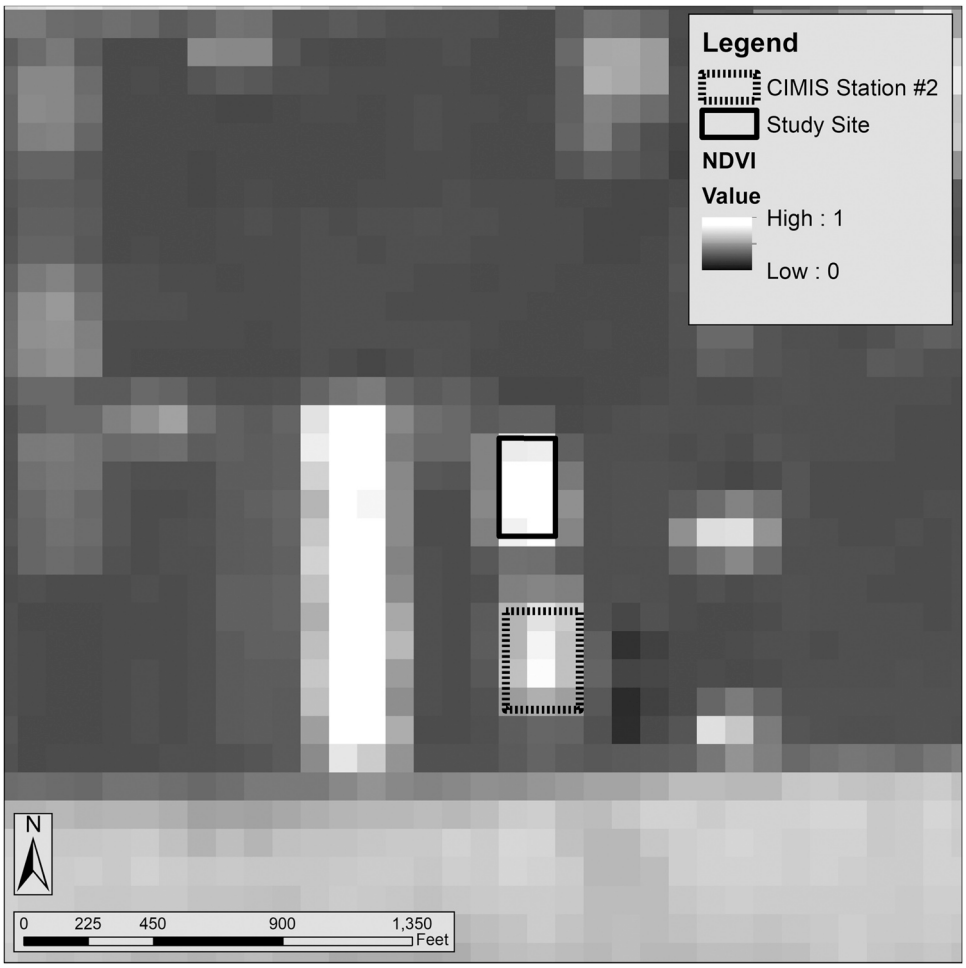

Fig. 4. NDVI from Landsat for the study site and surrounding area on June 2, 2015.

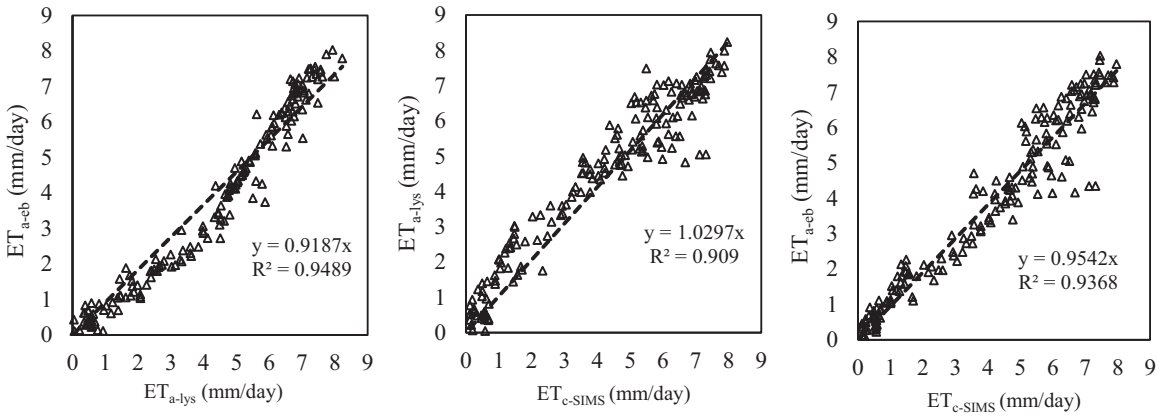

Fig. 5. (Left): Linear regression of ET measured by the REB station and weighing lysimeter. (Mid): Linear regression of ET measured by the REB station and remotely sensed by SIMS. (Right): Linear regression of ET measured by the weighing lysimeter and ET remotely sensed by SIMS. All comparison dates range from 1/1/2015 to 6/30/2015.

comparison between daily $ET_{c\text{-}SIMS}$ against $ET_{a\text{-}eb}$, $ET_{c\text{-}SIMS}$ had a small positive bias relative to $ET_{a\text{-}eb}$ (MBE of 0.15 mm/day), the model EF was high (0.93), MAE was only 0.47 mm/day and RMSE was 0.65 mm/day (Table 2).

3.2.2. *Intercomparison of evapotranspiration*

From the f_c data shown in Fig. 2, we estimated the lengths of crop stages and plotted linear regressions representing each growth stage. In the comparison between $ET_{c\text{-}SIMS}$ and $ET_{a\text{-}lys}$, a close relationship was obtained for both mid and late seasons, while an underestimation of $ET_{c\text{-}SIMS}$ was observed in the initial and crop establishment stage. The comparison between $ET_{c\text{-}SIMS}$ and $ET_{a\text{-}eb}$ showed that there was slight overestimation of $ET_{c\text{-}SIMS}$ for the mid-season. However, closer relationships between the two sets of data were observed in the initial and crop establishment stage and late seasons (Fig. 6). In Figs. 7 and 8, vertical lines were drawn to distinguish growth stages where the first

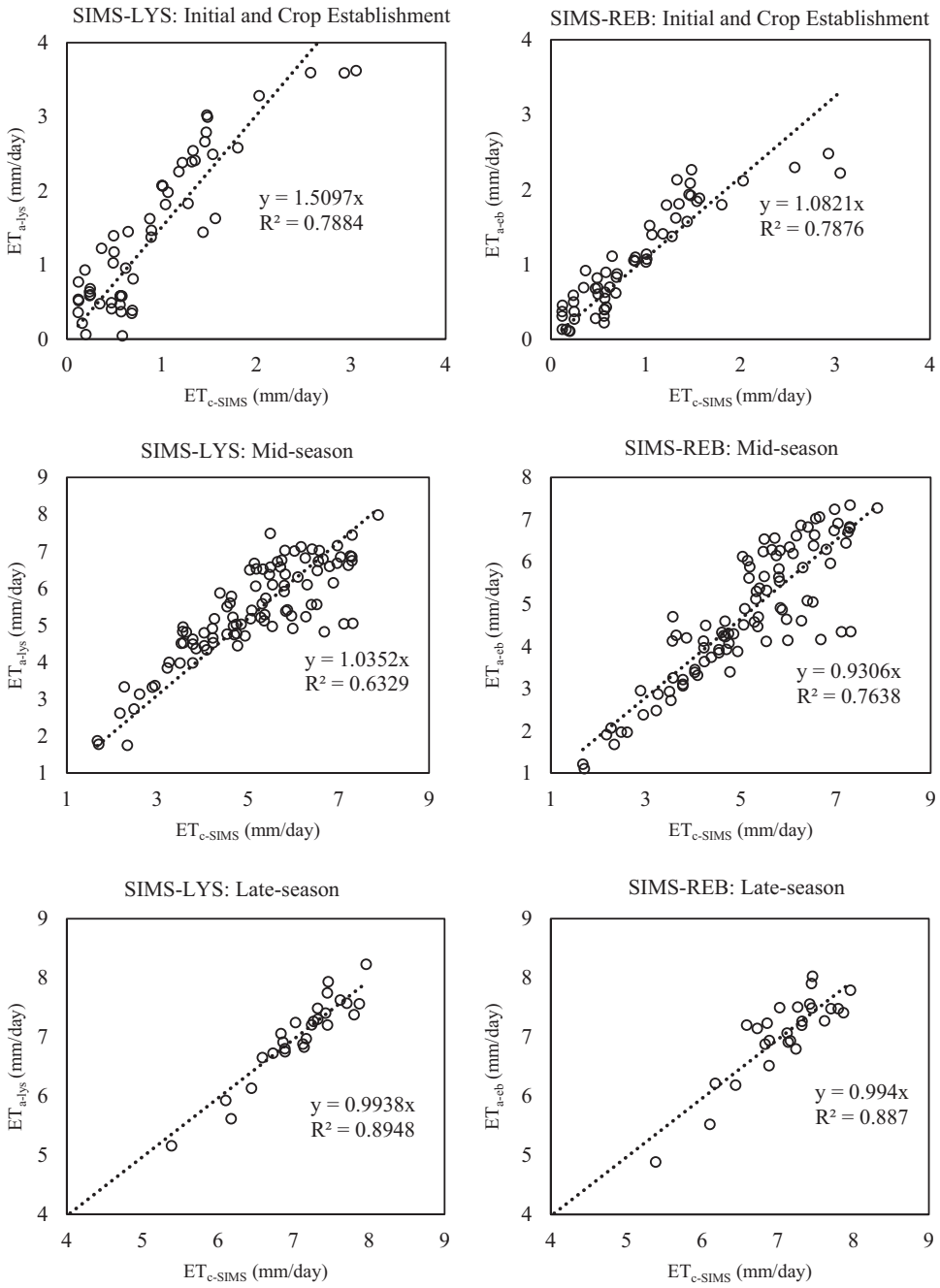

Fig. 6. Linear regressions of $ET_{c\text{-}SIMS}$ versus $ET_{a\text{-}lys}$ measured by weighing lysimeter and $ET_{a\text{-}eb}$ measured by the REB station. Comparisons are separated into different crop growth stages based on the fractional cover shown in Fig. 2.

Table 2
Statistical metrics comparing the daily ET measured by REB and weighing lysimeter with remotely sensed ET data from SIMS. For each comparison, we calculated Mean Bias Error (MBE); Mean Absolute Error (MAE); Root Mean Square Error (RMSE); and Modeling Efficiency (EF).

	$ET_{a\text{-}lys}$				$ET_{a\text{-}eb}$			
	MBE	MAE	RMSE	EF	MBE	MAE	RMSE	EF
$ET_{c\text{-}SIMS}$	−0.31 mm	0.56 mm	0.73 mm	0.91	0.15 mm	0.47 mm	0.65 mm	0.93

section is the initial and crop development stage (01/01/2015–02/26/2015); the second section is the mid-season (02/27/2015–06/02/2015); and the last section is the late season (06/03/2015–06/30/2015). On a daily timestep, $ET_{a\text{-}lys}$ and $ET_{a\text{-}eb}$ tracked closely with each other (Fig. 7). Over the development stage, the weighing lysimeter, in general, had the highest ET, and $ET_{a\text{-}lys}$ was consistently higher than $ET_{a\text{-}eb}$ and $ET_{c\text{-}SIMS}$, though agreement between these measurements increased as the crop reached maturity. $ET_{c\text{-}SIMS}$ was generally the lowest, likely due to the soil evaporation from exposed soil, which is only considered to a limited extent in $ET_{c\text{-}SIMS}$. As the canopy develops, transpiration becomes

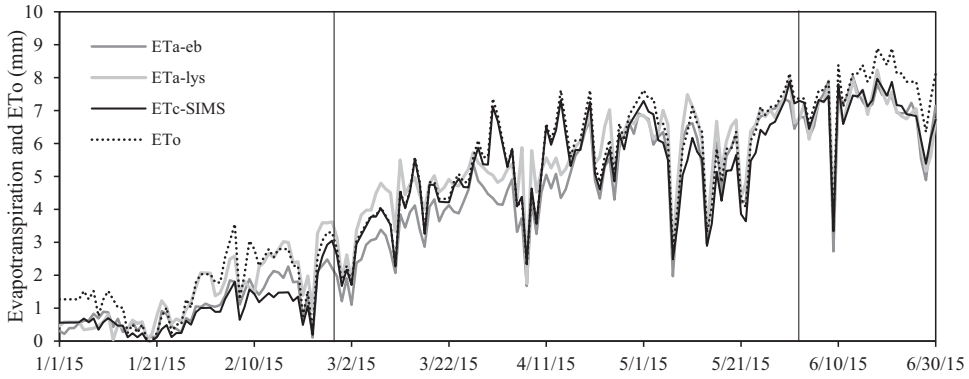

Fig. 7. Timeseries of daily $ET_{a\text{-}eb}$ calculated from the REB station measurements (dark gray), $ET_{a\text{-}lys}$ calculated from the weighing lysimeter (light gray), SIMS $ET_{c\text{-}SIMS}$ (black), and ET_o from CIMIS Station #2 (dotted-black) during the entire growing season. Vertical lines delineate the crop growth stages estimated from fractional cover.

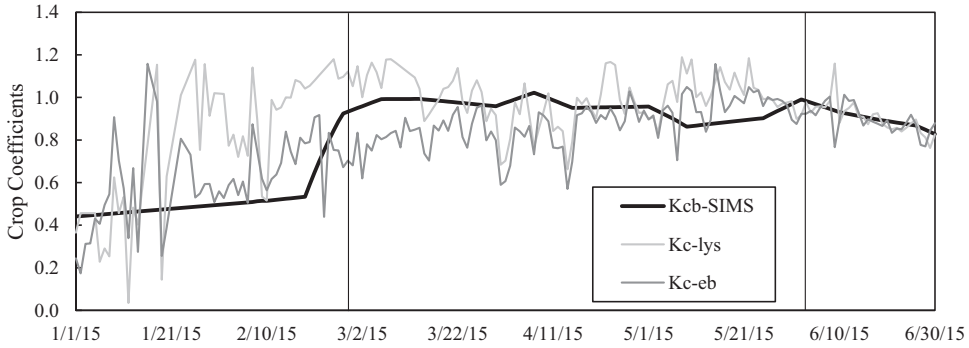

Fig. 8. Timeseries of the crop coefficients calculated from the REB station (dark gray), weighing lysimeter (light gray), and K_{cb} from SIMS (black) during the entire growing season. Vertical lines delineate the crop growth stages estimated from fractional cover.

dominant and increased alignment among all measurements was observed; e.g., during the mid-season and towards the end of the crop cycle, a max $ET_{c\text{-}SIMS}$ of 7.88 mm was observed on May 31st, compared to 7.98 mm for $ET_{a\text{-}lys}$ and 7.28 mm for $ET_{a\text{-}eb}$ (Fig. 7). During crop establishment, daily $ET_{c\text{-}SIMS}$ underestimated $ET_{a\text{-}lys}$ and $ET_{a\text{-}eb}$ by 51.0% and 8.2%, respectively. During mid-season, daily $ET_{c\text{-}SIMS}$ performed very well with an underestimation of 3.5% and an overestimation of 6.9% compared to $ET_{a\text{-}lys}$ and $ET_{a\text{-}eb}$, respectively. Similar patterns were observed in late season, where $ET_{c\text{-}SIMS}$ overestimated both $ET_{a\text{-}lys}$ and $ET_{a\text{-}eb}$ by 0.6% (Fig. 6), representing very strong agreement overall.

Daily $K_{c\text{-}lys}$ and $K_{c\text{-}eb}$ values were calculated from $ET_{a\text{-}lys}$ and $ET_{a\text{-}eb}$, by dividing the daily ET values by the daily ET_o from CIMIS station #2. Daily $K_{cb\text{-}SIMS}$ values were calculated through linear interpolation between the satellite-based K_{cb} values from SIMS calculated on satellite overpass dates. The daily K_c and K_{cb} timeseries from each of these data sources are plotted in Fig. 8. Over the entire study period, daily $K_{c\text{-}lys}$ and $K_{c\text{-}eb}$ measurements were noisy, while K_{cb} values from SIMS ($K_{cb\text{-}SIMS}$) stayed relatively smooth due to the dependence on satellite NDVI measurements which track crop canopy development. $K_{cb\text{-}SIMS}$ presented a relatively dynamic curve with a max $K_{cb\text{-}SIMS}$ of 1.02, highlighting the value of using satellite data to measure variations in crop canopy density and extent relative to idealized conditions. SIMS, accompanied by both the lysimeter and flux station, entered the mid-season ~15 days earlier than crop growth stages suggested in FAO56. This result illustrates the ability of satellite data to capture localized variability in rates of crop canopy development driven by variations in agronomic practices and interannual variability in weather conditions. During the mid- and late-season, when soil evaporation was low, $K_{cb\text{-}SIMS}$ aligned closely with $K_{c\text{-}}$

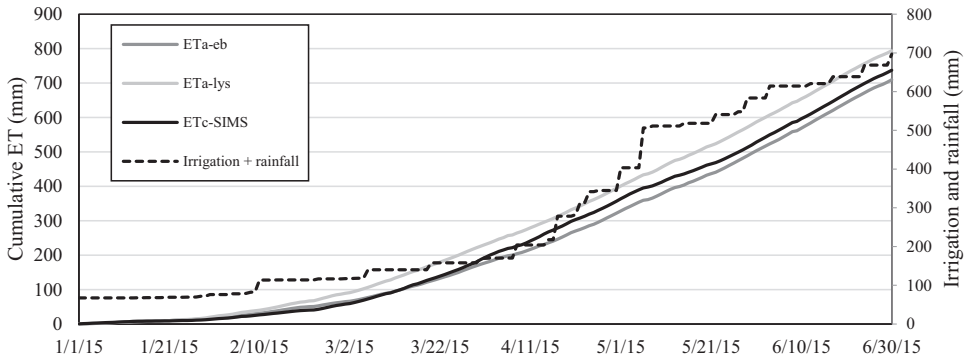

Fig. 9. The cumulative $ET_{a\text{-}eb}$ (dark gray), $ET_{a\text{-}lys}$ (light gray), and $ET_{c\text{-}SIMS}$ (black) over the study period. Available water from irrigation and rainfall is also included (dashed black). The first 67 mm of the available water represents the initial depth of water applied using sprinklers for crop establishment.

$_{lys}$ and $K_{c\text{-}eb}$ (Fig. 8).

The cumulative values of ET throughout the sugar beet crop cycle for the various sources are presented in Fig. 9. On the primary y-axis, the seasonal total of $ET_{a\text{-}lys}$ was 793.9 mm; $ET_{a\text{-}eb}$ was 709.6 mm; and $ET_{c\text{-}SIMS}$ was 737.1 mm. On the secondary y-axis, the total irrigation and precipitation was 696.6 mm. Seasonally, $ET_{c\text{-}SIMS}$ was 7.7% lower than $ET_{a\text{-}lys}$ and 3.7% higher than $ET_{a\text{-}eb}$. We also separated cumulative ET into corresponding crop stages. During initial and crop establishment, cumulative $ET_{c\text{-}SIMS}$, $ET_{a\text{-}lys}$, $ET_{a\text{-}eb}$ were 51.3 mm, 81.8 mm, and 59.9 mm, respectively; during mid-season, cumulative $ET_{c\text{-}SIMS}$, $ET_{a\text{-}lys}$, $ET_{a\text{-}eb}$ was 491.2 mm, 518.4 mm, and 456.6 mm, respectively; during late season, cumulative $ET_{c\text{-}SIMS}$, $ET_{a\text{-}lys}$, $ET_{a\text{-}eb}$ was 194.6 mm, 193.7 mm, and 193.1 mm, respectively.

4. Discussion

4.1. Comparison between ground measurements

During the growing season, the weighing lysimeter was carefully maintained to ensure data quality. Additionally, it was calibrated twice with high R^2 values of 0.9999 in December 2014 and 0.9998 in February 2015. This supported the accuracy and reliability of the measurements from the weighing lysimeter. Over the course of the study, daily average $ET_{a\text{-}eb}$ was 8% lower than $ET_{a\text{-}lys}$ (Fig. 5). Moorhead et al. (2019) reported similar findings for sorghum and corn with a daily underestimation of 14% using Eq. (8) with H calculated from a scintillometer. Although weighing lysimeters are generally considered to provide the most accurate characterization of ET (Howell et al., 1985; Evett et al., 2012), the WSREC weighing lysimeter, similar to most weighing lysimeters, has a calibrated irrigation system (1 mm of water/4 kg weight loss) and is maintained differently than the rest of the field. Compared to weighing lysimeters, REB is a portable and cost-effective alternative that captures a more complete spatial representation of the field. However, without the direct measurement of the latent energy flux, it is not possible to evaluate the energy balance closure, and thus difficult to evaluate the accuracy without a second independent measurement. By forcing closure, some of the storage terms are also neglected in the REB approach. In future studies, it would be preferable to employ an infrared gas analyzer to benchmark the REB approach across different crop types. Overall, when compared to the $ET_{a\text{-}lys}$ data at this site, $ET_{a\text{-}eb}$ agrees well, with underestimation of 11% at a seasonal timestep (Fig. 9), and a MAE of 8% at a daily timestep (Fig. 5). This level of agreement shows strong potential for use of the REB approach in water management applications when use of lysimetry or full OPEC instrumentation is not feasible.

4.2. Intercomparison and implications for K_{cb} from NDVI

The overall pattern in daily ET for the crop is summarized in Fig. 7. Daily ET peaked at approximately 8.23 mm/day and 8.55 mm/day for the weighing lysimeter and REB station, respectively. The timing of this peak corresponded with a maximum $ET_{c\text{-}SIMS}$ value of 7.96 mm/day. The maximum $K_{cb\text{-}SIMS}$ was 1.02, as shown in Fig. 8. Hauer et al. (2015) used field measured canopy height and f_c coupled with A&P approach and found a maximum K_{cb} of 1.12 for a sugar beet field. González-Dugo and Mateos (2008) derived a maximum K_{cb} (using a soil adjusted vegetation index (SAVI)) ranging from ~1.0–1.2 from four sugar beet fields. FAO56 Table 12 lists $K_{c\ mid}$ value of 1.2 and FAO56 Table 17 lists $K_{cb\ mid}$ value of 1.15 for sugar beet under well-watered conditions in sub-humid climates (Allen et al., 1998). The maximum $K_{cb\text{-}SIMS}$ compared well with these studies, although at the lower end. Following the period of maximum daily ET around June 18th, there is a sharp decline in $ET_{c\text{-}SIMS}$ and both sets of ground measurements, which correspond to the end of irrigation for the field and the onset of senescence of the crop (Figs. 7 and 8). This suggests that $K_{cb\text{-}SIMS}$ has the ability to accurately capture localized information, especially at the peak crop stage (Fig. 8). In addition, $K_{cb\text{-}SIMS}$ values throughout the crop cycle are within the range of values obtained by González-Dugo and Mateos (2008), where the VI based approach to estimate K_{cb} was also applied.

4.3. Strengths and limitations of SIMS

Due to the reliance primarily on measurement in the visible and near-infrared wavelengths, SIMS can be implemented using remote sensing data from a variety of satellite and airborne platforms including Landsat and Sentinel-2. Using data from multiple satellites, SIMS can currently update satellite-derived NDVI, f_c, and K_{cb} values every 4–5 days through the combined use of data from Landsat 8, Sentinel-2A and Sentinel-2B. Johnson et al. (2016) showed in field trials for lettuce and broccoli that use of SIMS data with other irrigation and nutrient management applications, such as CropManage developed by the University of California Agriculture and Natural Resources (UCANR) Institute, resulted in reductions in applied water of 20–40% relative to static irrigation schedules.

Daily $ET_{c\text{-}SIMS}$ considerably underestimated daily $ET_{a\text{-}lys}$ by 51.0% on average during the crop development stage (Fig. 6), which is likely due to the model's parametrizations of the diffusive evaporative component. This suggests that incorporation of a gridded soil water balance model to account for evaporation from bare soil via calculation of K_e values is necessary to help SIMS provide a better estimation of ET_c during the period of initial and crop establishment stages. During the mid- to late-season, good agreement was observed between each independent measurement of ET from the sugar beet field (Fig. 6). As reported in Glenn et al. (2011), the uncertainty between satellite-estimated ET and in-situ measurements can generally range from ~5–10% for lysimetry and ~10–30% for flux data. Similar results were found in Padilla et al. (2011), where they used a $K_{cb\text{-}VI}$ approach (complemented with a soil water balance for K_e and stress coefficient) to estimate ET in wheat and corn. Their modeled results compared well with both daily ET_a measured from EC and the lysimeter, with an average overestimation of 8%. Mateos et al. (2013) used a $K_{cb\text{-}VI}$ approach (in conditions of no water stress) in cotton and found their modeled results overestimated daily ET_a measured from EC by less than 10%. We found that the seasonal difference of $ET_{c\text{-}SIMS}$ was 7.7% lower than $ET_{a\text{-}lys}$ and 3.7% higher than $ET_{a\text{-}eb}$ (Fig. 9). The RMSE values for the comparison between $ET_{c\text{-}SIMS}$ and $ET_{a\text{-}lys}$ (0.73 mm, Table 2) and between $ET_{c\text{-}SIMS}$ and $ET_{a\text{-}eb}$ (0.65 mm, Table 2) are in agreement with RMSE reported (0.75 mm) in Mateos et al. (2013). The high modeling efficiency for the comparison: 1) between $ET_{a\text{-}lys}$ and $ET_{c\text{-}SIMS}$ (0.91); 2) between $ET_{a\text{-}eb}$ and $ET_{c\text{-}SIMS}$ (0.93) further indicates the good performance of SIMS (Table 2). These results suggest that SIMS is able to provide ET estimates within the expected range of uncertainty of the in-situ measurements. The close alignment of $ET_{c\text{-}SIMS}$ with $ET_{a\text{-}lys}$ and $ET_{a\text{-}eb}$ from mid- and late season (Figs. 6 and 7) further showcases that $K_{cb\text{-}SIMS}$, calculated using the A&P approach coupled with satellite-derived VI and f_c data, has the potential for operational ET estimation for irrigation management of sugar beets.

Although daily $ET_{c\text{-}SIMS}$ underestimated $ET_{a\text{-}lys}$ by only 2.97% throughout the whole growing period as shown in Fig. 5, the approach used to calculate $ET_{c\text{-}SIMS}$ from satellite-derived VI data misses soil evaporation during the crop establishment period (Fig. 7). Compared to daily average $ET_{a\text{-}lys}$, $ET_{c\text{-}SIMS}$ greatly underestimated ET by 51.0% during the crop establishment period, versus a 3.5% underestimation during mid-season and a 0.6% overestimation for end-season (Fig. 6). The underestimations during the initial and establishment periods suggest that the limitation of missing soil evaporation is evident; while the later close alignments confirm that $ET_{c\text{-}SIMS}$ agrees well with $ET_{a\text{-}lys}$ once the crop canopy is established, validating the use of K_{cb} from NDVI with A&P approach.

When compared to daily $ET_{a\text{-}eb}$, daily $ET_{c\text{-}SIMS}$ overestimated ET by 4.6% during the entire crop cycle (Fig. 5). Throughout crop stages, daily $ET_{c\text{-}SIMS}$ consistently overestimated $ET_{a\text{-}eb}$, except the 8.2% underestimation during the initial and crop establishment (Fig. 6). The

underestimation further proves the need to account for soil evaporation in the early stages. The later overestimations could be caused by flux measurements as any overestimations in H or underestimations in Rn and G would result an underestimation of λE based on Eq. (8). However, this is unknown due to the lack of determination of the energy balance closure, further highlighting the importance of having an independent measurement of λE along with other energy balance sensors.

Considering phenology directly influences evaporative rates, it could be beneficial to incorporate other climatic variables within SIMS since accurate estimations of K_{cb} are contingent on the crop growth stages (Richardson et al., 2013; Hunsaker et al., 2002). Although this study demonstrated strong alignment between SIMS and two independent field measurements of ET, variables including cumulative growing degree days (CGDD), derived by maximum, minimum, and base temperature, could be used to determine crop growth stages and better construct the K_{cb} curve for mid- and late-season in the future (Stegman, 1988; Slack et al., 1996; Raes et al., 2012). This has previously been done in studies such as Hunsaker et al. (2003a, 2003b), where they used CGDD in addition to NDVI to construct the K_{cb} curve ($R^2 = 0.82$) after full canopy cover (NDVI > 0.8). However, as advection can affect surface energy dynamics, it is important to distinguish a reasonable temperature threshold should CGDD be incorporated with NDVI.

5. Conclusion

The performance of SIMS for ET mapping was evaluated in a drip irrigated sugar beet field in the California Central Valley over a 181-day crop cycle. The accuracy of $ET_{c\text{-}SIMS}$ was assessed against ET data from a weighing lysimeter and a REB flux station. Daily $ET_{c\text{-}SIMS}$ data was derived from Landsat 8 surface reflectance data coupled with the A&P approach. Comparisons performed in this study for $ET_{c\text{-}SIMS}$ yielded an RMSE of 0.73 mm/day and 0.65 mm/day compared to $ET_{a\text{-}lys}$ and $ET_{a\text{-}eb}$, respectively. Seasonally, $ET_{c\text{-}SIMS}$ totaled 737.1 mm, which was within 7.7% of total $ET_{a\text{-}lys}$, and 3.7% of $ET_{a\text{-}eb}$.

Daily $ET_{c\text{-}SIMS}$ was 0.55 mm/day lower than daily $ET_{a\text{-}lys}$ on average, resulting in an underestimation relative to $ET_{a\text{-}lys}$ of 38.7 mm during the initial crop establishment period, highlighting the limited sensitivity of VI-based approaches to soil evaporation. Once the crop canopy began to develop, however, there was strong alignment between $ET_{c\text{-}SIMS}$ and $ET_{a\text{-}lys}$ with differences of only 0.25 mm/day as transpiration become the predominant component of ET. $ET_{c\text{-}SIMS}$ also agreed well during this period with $ET_{a\text{-}eb}$, with differences of −0.31 mm/day. $ET_{c\text{-}SIMS}$ also had better agreement with $ET_{a\text{-}eb}$ during the initial crop establishment period with differences of only 0.01 mm /day. Results from use of the REB approach in this study are promising and show reasonable overall agreement with the lysimeter measurement. In the future, deployment of an IRGA alongside the REB instrumentation would be important in benchmarking the performance of the REB approach before extensive use as the sole ground data source for assessment of remotely sensed ET estimates.

Acknowledging the underestimation of soil evaporation during the initial period of crop establishment, we conclude that $ET_{c\text{-}SIMS}$ is able to provide reasonable daily and seasonal estimates of ET_c for sugar beets, especially during the mid- and late-season. This assessment of SIMS further supports the utility of applying satellite VI-based methods coupled with the A&P approach to estimate ET_c for drip-irrigated crops. To address the underestimation of soil evaporation during the initial period of crop establishment, future studies should incorporate a gridded soil water balance model to support calculation of K_e to estimate soil evaporation within SIMS. Currently, SIMS is being implemented and validated for a wide range of crop types in the Salinas Valley and Central Valley in California, and ongoing work is supporting expansion across the western U.S. The ability of SIMS to rapidly estimate field scale ET_c via fully automated methods could be useful and significant to agricultural producers and water resource managers for future water use efficiency and conservation efforts.

Declaration of Competing Interest

The authors declare that they have no known competing financial interests or personal relationships that could have appeared to influence the work reported in this paper.

Acknowledgments

This research was supported with grants from the California State University Agricultural Research Institute (Award #16-01-103), and the NASA Applied Sciences Program Western Water Applications Office (Award #NNX12AD05A). Isabel Pôças acknowledges the Post-Doctoral grant supported by COMPETE 2020 and FCT (Award #POCI-01-0145-1092 FEDER-022217).

References

Abatzoglou, J.T., Ficklin, D.L., 2017. Climatic and physiographic controls of spatial variability in surface water balance over the contiguous United States using the Budyko relationship. Water Resour. Res. 53 (9), 7630–7643.
Allen, R.G., Pereira, L.S., Raes, D., Smith, M., 1998. Crop evapotranspiration - Guidelines for computing crop water requirements -. In: FAO Irrig. Drain. Pap., 56 FAO, Rome, p. 300p.
Allen, R.G., Tasumi, M., Trezza, R., 2007. Satellite-based energy balance for mapping evapotranspiration with internalized calibration (METRIC) - Model. J. Irrig. Drain. Eng. ASCE 133 (4), 380–394.
Allen, R.G., Pereira, L.S., 2009. Estimating crop coefficients from fraction of ground cover and height. Irrig. Sci. 28, 17–34.
Anapalli, S.S., Green, T.R., Reddy, K.N., Gowda, P.H., Sui, R., Fisher, D.K., Moorhead, J., Marek, G., 2018. Application of an energy balance method for estimating evapotranspiration in cropping systems. Agric. Water Manag. 204, 107–117.
Bastiaanssen, W.G.M., Menenti, M., Feddes, R.A., Holtslag, A.A.M., 1998. A remote sensing surface energy balance algorithm for land (SEBAL): 1. Formulation. J. Hydrol. 212–213, 198–212.
Bausch, W.C., 1993. Soil background effects on reflectance-based crop coefficients for corn. Remote Sens. Environ. 46 (2), 213–222.
Bausch, W.C., Neale, C.M.U., 1987. Crop coefficients derived from reflected canopy radiation: a concept. Trans. ASAE 30 (3), 703–709.
Benedetti, R., Rossini, P., 1993. On the use of NDVI profiles as a tool for agricultural statistics: the case study of wheat yield estimate and forecast in Emilia Romagna. Remote Sens. Environ. 45 (3), 311–326.
Bryla, D.R., Trout, T.J., Ayars, J.E., 2010. Weighing lysimeters for developing crop coefficients and efficient irrigation practices for vegetable crops. HortScience 45, 1597–1604.
Burba, G., 2001. Illustration of Flux Footprint Estimates affected by Measurement Height, Surface Roughness, and Thermal Stability. Automated Weather Stations for Applications in Agriculture and Water Resources Management: Current Use and Future Perspectives. World Meteorological Organization,, Lincoln, NE.
Businger, J.A., 1986. Evaluation of the accuracy with which dry deposition can be measured with current micrometeorological techniques. J. Clim. Appl. Meteorol. 25 (8), 1100–1124.
Calera, A., Campos, I., Osann, A., D'Urso, G., Menenti, M., 2017. Remote sensing for crop water management: from ET modelling to services for the end users. Sensors ((Switzerland)) 17 (5), 1104.
Campos, I., Villodre, J., Carrara, A., Calera, A., 2013. Remote sensing-based soil water balance to estimate Mediterranean holm oak savanna (dehesa) evapotranspiration under water stress conditions. J. Hydrol. 494, 1–9.
, 2007110th Congress, 2007. Energy Independence and Security Act of 2007, Public Law.
Drerup, P., Brueck, H., Scherer, H.W., 2017. Evapotranspiration of winter wheat estimated with the FAO 56 approach and NDVI measurements in a temperate humid climate of NW Europe. Agric. Water Manag. 192, 180–188.
Evett, S.R., Schwartz, R.C., Howell, T.A., Louis Baumhardt, R., Copeland, K.S., 2012. Can weighing lysimeter ET represent surrounding field ET well enough to test flux station measurements of daily and sub-daily ET? Adv. Water Resour. 50, 79–90.
Gash, J.H.C., 1986. A note on estimating the effect of a limited fetch on micrometeorological evaporation measurements. Bound.-Layer Meteorol. 35, 409–413.
Glenn, E.P., Huete, A.R., Nagler, P.L., Hirschboeck, K.K., Brown, P., 2007. Integrating remote sensing and ground methods to estimate evapotranspiration. CRC Crit. Rev. Plant Sci. 26 (3), 139–168.
Glenn, E.P., Neale, C.M.U., Hunsaker, D.J., Nagler, P.L., 2011. Vegetation index-based crop coefficients to estimate evapotranspiration by remote sensing in agricultural and natural ecosystems. Hydrol. Process 25, 4050–4062.
González-Dugo, M.P., Mateos, L., 2008. Spectral vegetation indices for benchmarking water productivity of irrigated cotton and sugarbeet crops. Agric. Water Manag. 95 (1), 48–58.
Goward, S.N., Markham, B., Dye, D.G., Dulaney, W., Yang, J., 1991. Normalized difference vegetation index measurements from the advanced very high resolution radiometer. Remote Sens. Environ. 35 (2–3), 257–277.

Hart, Q.J., Brugnach, M., Temesgen, B., Rueda, C., Ustin, S.L., Frame, K., 2009. Daily reference evapotranspiration for California using satellite imagery and weather station measurement interpolation. Civ. Eng. Environ. Syst. 26 (1), 19–33.
Hauer, M., Koch, H.J., Märländer, B., 2015. Water use efficiency of sugar beet cultivars (Beta vulgaris L.) susceptible, tolerant or resistant to Heterodera schachtii (Schmidt) in environments with contrasting infestation levels. Field Crop. Res. 183, 364–365.
Horst, T.W., Weil, J.C., 1994. How far is far enough? The fetch requirements for micrometeorological measurement of surface fluxes. J. Atmos. Ocean. Technol. 11 (4), 1018–1025.
Howell, T.A., McCormick, R.L., Phene, C.J., 1985. Design and installation of large weighing lysimeters. Trans. ASAE 28 (1), 106–112.
Hunsaker, D.J., Pinter, P.J., Cai, H., 2002. Alfalfa basal crop coefficients for FAO-56 procedures in the desert regions of the Southwestern U.S. Trans. Am. Soc. Agric. Eng. 45 (6), 1799–1815.
Hunsaker, D.J., Pinter, P.J., Barnes, E.M., Kimball, B.A., 2003a. Estimating cotton evapotranspiration crop coefficients with a multispectral vegetation index. Irrig. Sci. 22, 95–104.
Hunsaker, D.J., Fitzgerald, G.J., French, A.N., Clarke, T.R., Ottman, M.J., Pinter, P.J., 2007a. Wheat irrigation management using multispectral crop coefficients: I. Crop evapotranspiration prediction. Trans. ASABE 50 (6), 2017–2033.
Hunsaker, D.J., Fitzgerald, G.J., French, A.N., Clarke, T.R., Ottman, M.J., Pinter, P.J., 2007b. Wheat irrigation management using multispectral crop coefficients: II. Irrigation scheduling performance, grain yield, and water use efficiency. Trans. ASABE 50 (6), 2035–2050.
Hunsaker, D.J., Pinter, P.J., Barnes, E.M., Kimball, B.A., 2003b. Estimating cotton evapotranspiration crop coefficients with a multispectral vegetation index. Irrig. Sci. 22 (2), 95–104.
Hunsaker, D.J., Pinter, P.J., Kimball, B.A., 2005. Wheat basal crop coefficients determined by normalized difference vegetation index. Irrig. Sci. 24, 1–14.
Johnson, L.F., Trout, T.J., 2012. Satellite NDVI assisted monitoring of vegetable crop evapotranspiration in California's San Joaquin Valley. Remote Sens. 4 (2), 439–455.
Johnson, L.F., Cahn, M., Martin, F., Melton, F., Benzen, S., Farrara, B., Post, K., 2016. Evapotranspiration-based irrigation scheduling of head lettuce and broccoli. HortScience 51 (7), 935–940.
Kaffka, S.R., Zhang, T.G., Yeo, B.-L., Yang, W.-R., 2014. 74 th IIRB Congress-74 ème Congrès de l'IIRB-74, IIRB-Kongress, 14.
Kjaersgaard, J., Allen, R., Irmak, A., 2011. Improved methods for estimating monthly and growing season ET using METRIC applied to moderate resolution satellite imagery. Hydrol. Process 25 (26), 4028–4036.
Kumar, K., Rosen, C.J., Gupta, S.C., 2002. Kinetics of nitrogen mineralization in soils amended with sugar beet processing by-products. Commun. Soil Sci. Plant Anal. 33 (19–20), 3635–3651.
Kustas, W.P., Norman, J.M., Schmugge, T.J., Anderson, M.C., 2004. Mapping surface energy fluxes with radiometric temperature. In: Quattrochi, D., Luvall, J. (Eds.), Thermal Remote Sensing in Land Surface Processes. CRC Press, Boca Raton, Florida, USA, pp. 205–253.
Linquist, B., Snyder, R., Anderson, F., Espino, L., Inglese, G., Marras, S., Moratiel, R., Mutters, R., Nicolosi, P., Rejmanek, H., Russo, A., Shapland, T., Song, Z., Swelam, A., Tindula, G., Hill, J., 2015. Water balances and evapotranspiration in water- and dry-seeded rice systems. Irrig. Sci. 33, 375–385.
Mateos, L., González-Dugo, M.P., Testi, L., Villalobos, F.J., 2013. Monitoring evapotranspiration of irrigated crops using crop coefficients derived from time series of satellite images. I. Method validation. Agric. Water Manag. 125, 81–91.
McElrone, A.J., Shapland, T.M., Calderon, A., Fitzmaurice, L., Paw, U., K.T, Snyder, R.L., 2013. Surface renewal: an advanced micrometeorological method for measuring and processing field-scale energy flux density data. J. Vis. Exp. 82, e50666.
Melton, F.S., Johnson, L.F., Guzman, A., Wang, T., Carrara, W., Hang, M., Doherty, C., 2020. The Satellite Irrigation Management Support System User's Manual and Algorithms. NASA Ames Research Center (accessed 26 May 2020). http://github.com/aguzman/sims/documentation/sims_user_manual.pdf.
Melton, F.S., Johnson, L.F., Lund, C.P., Pierce, L.L., Michaelis, A.R., Hiatt, S.H., Guzman, A., Adhikari, D.D., Purdy, A.J., Rosevelt, C., Votava, P., Trout, T.J., Temesgen, B., Frame, K., Sheffner, E.J., Nemani, R.R., 2012. Satellite irrigation management support with the terrestrial observation and prediction system: a framework for integration of satellite and surface observations to support improvements in agricultural water resource management. IEEE J. Sel. Top. Appl. Earth Obs. Remote Sens. 5 (6), 1709–1721.
Melton, F.S., Johnson, L.F., Guzman, A., Dexter, J., Zaragosa, I., Wang, T., Patron, E., Duque, J., Rosevelt, C., Cahn, M., Smith, R., Temesgen, B., Trezza, R., Eching, S., Frame, K., 2018. The Satellite Irrigation Management Support (SIMS) System: Applications of satellite Data to Support Improvements in Irrigation Management in California. California Plant and Soil Conference, American Society of Agronomy, pp. 49–51.
Meyers, T., Baldocchi, D., 2005. Current micrometeorological flux methodologies with applicationsin agriculture. Publ. Agencies Staff U. S. Dep. Commer 47, 381–396.
Moorhead, J.E., Marek, G.W., Gowda, P.H., Lin, X., Colaizzi, P.D., Evett, S.R., Kutikoff, S., 2019. Evaluation of evapotranspiration from eddy covariance using large weighing lysimeters. Agronomy 9 (2), 99.
Murray, R.S., Nagler, P.L., Morino, K., Glenn, E.P., 2009. An empirical algorithm for estimating agricultural and riparian evapotranspiration using MODIS enhanced vegetation index and ground measurements of ET. II. application to the lower Colorado river, U.S. Remote Sens. 1 (4), 1125–1138.
Odi-Lara, M., Campos, I., Neale, C.M.U., Ortega-Farías, S., Poblete-Echeverría, C., Balbontín, C., Calera, A., 2016. Estimating evapotranspiration of an apple orchard using a remote sensing-based soil water balance. Remote Sens. 8 (3), 253.
Padilla, F.L.M., González-Dugo, M.P., Gavilán, P., Domínguez, J., 2011. Integration of vegetation indices into a water balance model to estimate evapotranspiration of wheat and corn. Hydrol. Earth Syst. Sci. 15, 1213–1225.
Pan, X., Liu, Y., Fan, X., Gan, G., 2017. Two energy balance closure approaches: applications and comparisons over an oasis-desert ecotone. J. Arid Land 9, 51–64.
Panella, L., Kaffka, S.R., 2010. Sugar beet (Beta vulgaris L) as a biofuel feedstock in the United States. ACS Symp. Series 105, 163–175.
Panella, L., Kaffka, S.R., Lewellen, R.T., Mitchell McGrath, J., Metzger, M.S., Strausbaugh, C.A., 2015. Sugarbeet. John Wiley & Sons, Ltd,, pp. 357–395.
Pereira, L.S., Allen, R.G., Smith, M., Raes, D., 2015. Crop evapotranspiration estimation with FAO56: past and future. Agric. Water Manag. 147, 4–20.
Pereira, L., Paredes, P., Melton, F., Johnson, L., Wang, T., López-Urrea, R., Cancela, J., Allen, R., 2020. Prediction of crop coefficients from fraction of ground cover and height. Background and validation using ground and remote sensing data. Agric. Water Manag. 241, 106197.
Pôças, I., Paço, T.A., Paredes, P., Cunha, M., Pereira, L.S., 2015. Estimation of actual crop coefficients using remotely sensed vegetation indices and soil water balance modelled data. Remote Sens. 7 (3), 2373–2400.
Pôças, I., Calera, A., Campos, I., Cunha, M., 2020. Remote sensing for estimating and mapping single and basal crop coefficientes: a review on spectral vegetation indices approaches. Agric. Water Manag. 233, 106081.
Raes, D., Steduto, P., Hsiao, T.C., Fereres, E., 2012. AquaCrop Version 4.0 Reference Manual. FAO Land and Water Division,, Rome, p. 125.
Rafn, E.B., Contor, B., Ames, D.P., 2008. Evaluation of a method for estimating irrigated crop-evapotranspiration coefficients from remotely sensed data in Idaho. J. Irrig. Drain. Eng. 134 (6), 722–729.
Richardson, A.D., Keenan, T.F., Migliavacca, M., Ryu, Y., Sonnentag, O., Toomey, M., 2013. Climate change, phenology, and phenological control of vegetation feedbacks to the climate system. Agric. For. Meteorol. 169, 156–173.
Samani, Z., Bawazir, A.S., Bleiweiss, M., Skaggs, R., Longworth, J., Tran, V.D., Pinon, A., 2009. Using remote sensing to evaluate the spatial variability of evapotranspiration and crop coefficient in the lower Rio Grande Valley, New Mexico. Irrig. Sci. 28 (1), 93–100.
Semmens, K.A., Anderson, M.C., Kustas, W.P., Gao, F., Alfieri, J.G., McKee, L., Prueger, J. H., Hain, C.R., Cammalleri, C., Yang, Y., Xia, T., Sanchez, L., Mar Alsina, M., Vélez, M., 2016. Monitoring daily evapotranspiration over two California vineyards using Landsat 8 in a multi-sensor data fusion approach. Remote Sens. Environ. 185, 155–170.
Shapland, T.M., McElrone, A.J., Paw, U., K.T, Snyder, R.L., 2013. A Turnkey data logger program for field-scale energy flux density measurements using eddy covariance and surface renewal. Ital. J. Agrometeorol. 18 (1), 5–16.
Slack, D.C., Martin, E.C., Sheta, A.E., Fox Jr., F., Clark, L.J., Ashley, R.O., 1996. Crop coefficients normalized for climatic variability with growing-degree-days. In: Camp, C.R., Sadler, E.J., Yoder, R.E. (Eds.), Evapotranspiration and Irrigation Scheduling: Proceedings of an International Conference, 3–6 November 1996. ASAE, San Antonio, Texas and St Joseph, Michigan, pp. 892–898.
Stegman, E.C., 1988. Corn crop curve comparisons for the Central and Northern Plains of the U.S. Appl. Eng. Agric. 4, 226–233.
Swinbank, W.C., 1951. The measurement of vertical transfer of heat and water vapor of eddies in the lower atmosphere. J. Meteorol. 8 (3), 135–145.
Tanner, C.B., Thurtell, G.W., 1969. Anemoclinometer measurements of Reynolds stress and heat transport in the atmosphere surface layer, University of Wisconsin, Tech. Rep., ECOM-66-G22-F, 82PP. [Available from US Army Electronic Command, Atmospheric Sciences Laboratory, Ft. Huachuca, AZ 85613].
Tanner, B.D., 1988. Use requirements for Bowen ratio and eddy correlation determination of evapotranspiration. In: Hay, D.R. (Ed.), Planning Now for Irrigation and Drainage in the 21st Century, Proc., Irrig. and Drain. Div, Conf. ASCE, Lincoln, NE, USA, pp. 605–616.
Tasumi, M., Allen, R.G., 2007. Satellite-based ET mapping to assess variation in ET with timing of crop development. Agric. Water Manag. 88 (1–3), 54–62.
Thao, T., 2017. Developing Crop Coefficients (K_c) for Sugar Beet (*Beta vulgaris* L.) Grown Under Drip Irrigation using Weighing Lysimeters (MS Thesis). California State University,, Fresno.
Trout, T.J., Johnson, L.F., Gartung, J., 2008. Remote sensing of canopy cover in horticultural crops. HortScience 43 (2), 33–337..
Twine, T.E., Kustas, W.P., Norman, J.M., Cook, D.R., Houser, P.R., Meyers, T.P., Prueger, J.H., Starks, P.J., Wesely, M.L., 2000. Correcting eddy-covariance flux underestimates over a grassland. Agric. For. Meteorol. 103 (3), 279–300.